Available online at www.sciencedirect.com
ScienceDirect
Atmospheric Environment 40 (2006) 7953–7962
ATMOSPHERIC ENVIRONMENT
www.elsevier.com/locate/atmosenv

Sulfate aerosols forcing: An estimate using a three-dimensional interactive chemistry scheme

Sunita Verma[a,*], O. Boucher[b], H.C. Upadhyaya[a], O.P. Sharma[a]

[a]*Centre for Atmospheric Sciences, Indian Institute of Technology Delhi, New Delhi -110016, India*
[b]*Laboratoire d'Optique Atmosphérique, Université des Sciences et Technologies de Lille, Villeneuve d'Ascq, France*

Received 2 August 2005; received in revised form 5 July 2006; accepted 5 July 2006

Abstract

The tropospheric sulfate radiative forcing has been calculated using an interactive chemistry scheme in LMD-GCM. To estimate the radiative forcing of sulfate aerosol on climate, a consistent interaction between atmospheric circulation and radiation computation has been allowed in LMD-GCM. The model results indicate that the change in the sulfate aerosols number concentration is negatively correlated to the indirect radiative forcing. The model simulated annual mean direct radiative forcing ranges from -0.1 to $-1.2\,W\,m^{-2}$, and indirect forcing ranges from -0.4 to $-1.6\,W\,m^{-2}$. The global annual mean direct effect estimated by the model is $-0.48\,W\,m^{-2}$, and that of indirect is $-0.68\,W\,m^{-2}$.

Keywords: Sulfate aerosols; Radiative forcing; Cloud droplet number concentration; Direct forcing; Indirect forcing

1. Introduction

The issue of climate change, in general, and of the impact of human activity on climate, in particular, is the subject of the extensive analysis and assessment by the scientific community. Aerosols influence the Earth's radiation balance directly and indirectly by reflection of sunlight back to space and the interaction of particles with clouds (Twomey, 1974; Jones et al., 1994; Kiehl and Briegleb, 1993). The composition and distribution of atmospheric aerosols represent one of the largest uncertainties in our current understanding of Earth's climate. IPCCs best estimate of the sulfate direct radiative forcing is $-0.4\,W\,m^{-2}$ with a range of -0.2 to $0.8\,W\,m^{-2}$. The uncertainties relating to aerosol radiative forcings however remain large, and rely to a large extent on the estimates from global modelling. Most of the previous efforts to study the radiative forcing of aerosols in three-dimensional GCMs (e.g., Kiehl and Briegleb, 1993; Boucher and Anderson, 1995; Haywood et al., 1997a; Lohmann and Feichter, 1997; Lohmann et al., 2000; Ramaswamy et al., 2001); lacks in considering the feedback of aerosols on microphysics and therefore neglect the effects associated with evolution of species concentration with the evolving meteorology. To provide a sound basis for delineating the changes of anthropogenic influences on climate with reasonable fidelity, it is essential that aerosol radiative forcing be well quantified and accurately represented in climate models. The global chemistry models that are capable of resolving the

*Corresponding author.
E-mail address: verma.sunita@gmail.com (S. Verma).

1352-2310/$ - see front matter © 2006 Published by Elsevier Ltd.
doi:10.1016/j.atmosenv.2006.07.010

aerosol size distribution, cloud microphysics and state of mixing, allowing the calculation of the radiative effects from physical principles serve as an important tool for studying the anthropogenic influences.

The estimation of direct and indirect radiative forcing (IRF) by sulfate aerosols is attempted in this study using an interactive chemistry GCM with cloud related properties and aerosol. The prediction of cloud droplet number concentration (CDNC) is achieved from the number concentration of sulfate aerosol and cloud properties; hence the model design internally resolves the CDNC to the changes in the cloud water and aerosol parameters. In particular, this model considers an interactive scheme for feedback from chemistry to meteorology with internally resolving microphysical properties of aerosols for radiative transfer computations. Thus, it is a step towards correcting the deficiencies where the microphysics and feedbacks are run off-line to calculate the indirect effect of aerosols.

2. Model description

The radiative forcing is calculated using the Laboratoire de Météorologie Dynamique (LMD) general circulation model (Sadourny and Laval, 1984; Le Treut et al., 1994; Li, 1999; Lott, 1999) with aerosol simulation (Boucher et al., 1998; Boucher et al., 2002; Reddy et al., 2005). An important addition to LMD in the current version is the inclusion of a prognostic sulfur-cycle scheme. The sulfur chemistry has been independently developed from that of Boucher and Pham (2002), Boucher et al. (2002) and Hauglustaine et al. (2004). The newly implemented interactive sulfur chemistry scheme in the LMD-GCM has been fully described and thoroughly validated for atmospheric oxidants and sulfur species against measurements over different regions of the world (Verma et al., 2006). The annual sulfur cycle for global simulations has been analyzed for surface/horizontal distribution and inter-hemispheric transport. The same model setup has been successfully employed to simulate the sulfate aerosols for the INDOEX campaign. Results of this model have been compared with measurements for physical, optical, and radiative properties of sulfate (Verma et al., 2005) for INDOEX region. The chemistry module in the model includes all major chemical mechanisms for formation of atmospheric oxidants and sulfate. The chemical species and short-lived oxidant fields evolve interactively with meteorology to allow the complex interaction between chemistry and climate to consider the role of sulfate aerosols on climate system. The interactive gas phase in this model version is fully coupled with aerosol module, which provides aerosol mass and number distribution. The aerosol module is taken from the Community Multiscale Air Quality (CMAQ) model of Binkowski and Shankar (1995), which is also a part of Model-3 (Binkowski and Roselle., 2003) of US Environment Protection Agency (EPA).

2.1. Optical properties and radiative forcing

Aerosol microphysical and optical properties are important linking parameters to understand the radiative effects of aerosols on the climate. To effectively quantify the radiative effects, first, spectrally resolved optical properties (e.g., mass extinction coefficient, optical depth, single scattering albedo and asymmetry factor) of different aerosols must be computed. Second, these properties must be averaged over the spectral bands of the radiative transfer model in which they will be used. Finally, the variations of the optical properties with relative humidity (RH) must be parameterized to allow efficient use within the online chemistry and climate models. The direct and indirect forcing is calculated every 2 h time step based on the instantaneous model calculated sulfate mixing-ratios.

2.1.1. Direct effect

The radiative code in the LMD-GCM consists of improved versions of parameterizations of Fourquart and Bonnel (1980) for solar radiation and Morcrette (1999) for terrestrial radiation. The optical properties are obtained from Mie theory by using a size distribution and refractive indices of sulfate aerosols. In the radiative code of LMD, the shortwave spectrum is divided into two wavebands: 0.25–0.68 and 0.68–4.0 μm. The model accounts for the diurnal cycle of solar radiation and allows fractional cloudiness to form in a grid box. The shortwave radiative fluxes at the top of atmosphere (TOA) and at the surface are computed every 2 h with or without the presence of clouds and aerosols. The clear-sky and all-sky radiative forcing are estimated as the difference in shortwave radiative fluxes with and without aerosols.

Optical properties are computed over the entire shortwave spectrum (0.25–4.0 μm) at 24 wave-

lengths and grouped into the two model wavebands as weighted averages with a typical spectral distribution of the incoming solar radiation flux at the surface. The aerosols take up water and grow in size with RH. Thus, RH affects both the particle size and density of sulfate aerosols. Aerosol optical depth (AOD) information can be readily used to estimate the aerosol radiative forcing. The sulfate AOD (τ^a) in the model is estimated as

$$\tau_a^l = \alpha_e M_l \Delta Z_l, \quad (1)$$

where α_e is the extinction efficiency, M_l is the mass of sulfate aerosol in a layer of thickness ΔZ_l here and subscript l denotes any particular model layer.

2.1.2. Indirect effect

Aerosols serve as cloud condensation and ice nuclei. An increase in aerosol concentration and or properties can therefore modify the microphysical properties of clouds, as well as precipitation efficiency and hence the cloud lifetime. The indirect forcing is calculated by Jones et al. (1994) formulation. The sulfate mass is empirically related to CDNC (N_d) as

$$N_d = \mathrm{MAX}\{3.75 \times 10^8 (1 - \exp[-2.5 \times 10^{-9} N_j]), N_{min}\}, \quad (2)$$

where N_j is the sulfate number concentration in the accumulation mode and N_{min} has been set to a value $5 \times 10^6\ m^{-3}$. The droplet number N_d obtained from (2) is then used for calculating the effective radius of cloud drop (r_e) in the model, which is further used to calculate the cloud optical thickness (τ);

$$\tau = \frac{3W}{2\rho_w r_e}, \quad (3)$$

where W represents the cloud liquid path and ρ_w is the density of water in (3). The scheme requires knowledge of optical depth, asymmetry parameter and single scattering albedo of cloud in each of two bands. Distinction between liquid and ice water is temperature based on liquid and ice clouds between 0° and −40 °C. The effective radius of cloud droplet (r_e) is calculated from the radii of warm and ice clouds. The cloud emissivity (ε) used in the longwave calculations is computed in the model as

$$\varepsilon = (1 - e^{-\kappa})W. \quad (4)$$

The absorption coefficient (κ) is set equal to 0.13 ($m^2\,g^{-1}$) for all cloud types.

3. Design of experiments

Radiative effects of sulfate aerosols are estimated using LMD-GCM by assuming two sulfur emission scenarios; a pre-industrial scenario and present-day scenario. The pre-industrial simulation represents the sulfur emissions before industrial revolution

Table 1
Global annual sulfur emissions for pre-industrial and present-day (Tg S yr^{-1})

Sources	Present day simulations	Pre-industrial simulations
Biosphere	0.70	0.70
Biomass-burning	2.99	2.99
Oceanic	16.30	16.30
Man-made	67.73	0.0
Total	87.72	19.99

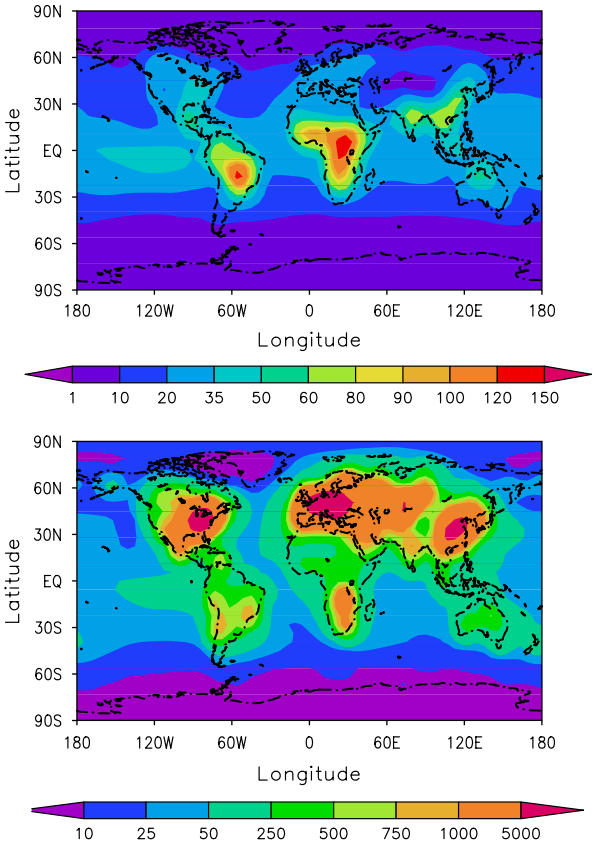

Fig. 1. Annual mean surface SO_2 concentrations (pptv) in pre-industrial (upper panel) and present-day (lower panel) simulations.

and present-day simulation refers to the sulfur emissions for mid-1990. These experiments help to estimate the anthropogenic sulfate forcing. The simulations differ only in terms of anthropogenic sulfur emissions.

3.1. Emissions

The pre-industrial scenario uses only natural emission of sulfur from GEIA database and the anthropogenic emissions are set to zero (pre-industrial state). The present-day scenario (Table 1) includes the natural as well as anthropogenic emissions (present day).

3.1.1. Present day simulations

The emissions are taken from GEIA inventory (Table 1). The global total of man-made sources is 67.73 Tg S yr^{-1}. We consider both natural as well as anthropogenic sulfur emissions in the present-day simulations (Table 1). We assume 95% of sulfur emissions in the form of SO_2 and remaining 5% are directly emitted as sulfate in accumulation mode.

3.1.2. Pre-industrial simulations

Only biogenic sources of sulfur emissions are considered. DMS is the main sulfur biogenic compound emitted to the atmosphere from the open ocean waters. The global source strength of 16.59 Tg S yr^{-1} of DMS is used in the model, which is in the range of previous estimates by Bates et al. (1992) and Spiro et al. (1992). Table 1 gives the summary of the yearly global integrated fluxes of each sulfur compounds for both simulations. The main biogenic source is ocean and it contributes to 83% of total source.

4. Numerical simulations

Simulations are carried out for five years using an interactive chemistry LMD-GCM. Forcing is calculated from the fluxes averaged over the last one-year

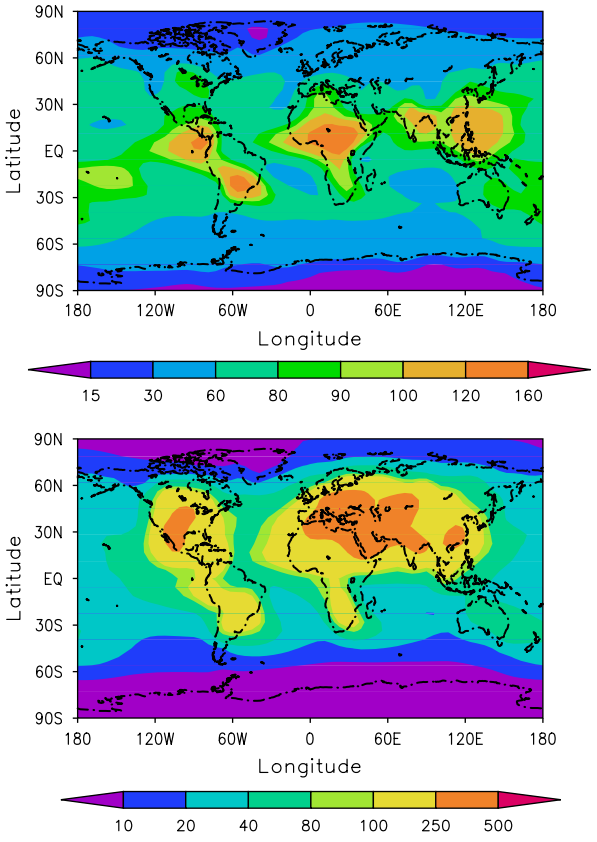

Fig. 2. Annual mean sulfate column burden (pptv) in pre-industrial (upper panel) and present-day (lower panel) simulations.

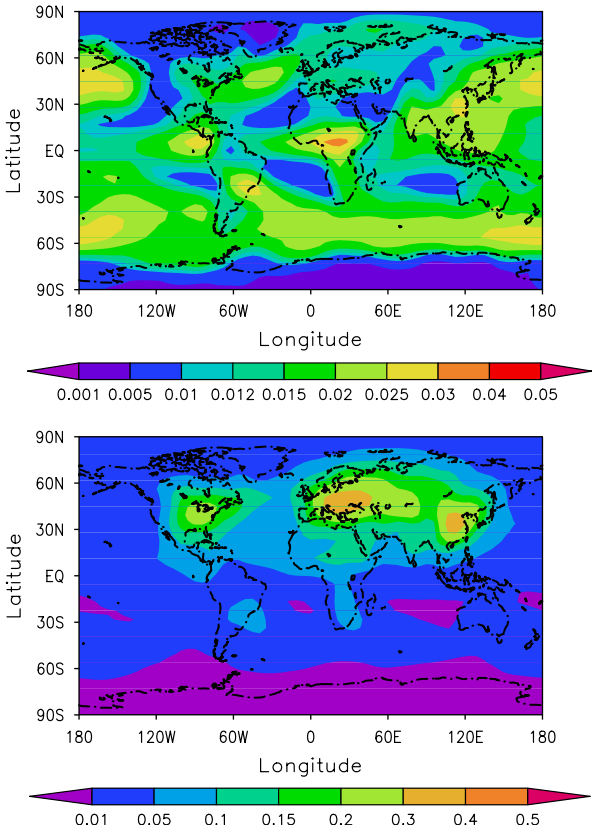

Fig. 3. Annual mean sulfate aerosol optical depth in pre-industrial (upper panel) and present-day (lower panel) simulations.

duration of the simulation period. The same meteorological fields are used in both simulations. Since the main aim here is to calculate differences in the radiative forcing (RF) arising from the present-day and pre-industrial emissions, the sequence of calculations is important. Only the first indirect effect has been considered for which parameterization of Jones et al. (1994) has been used. The relationship (2) has been used to compute CDNC in droplets per cm^{-3} from the sulfate mass. For the first indirect effect of aerosols, the shortwave radiation calculations are performed every 2 h, once with cloud droplet concentration (and cloud radius and optical depth) calculated from all sulfate aerosols and next with the same quantities calculated from natural sulfate aerosols only. Thus, RFs are computed as the differences in the TOA shortwave radiative flux between two simulations, with and without anthropogenic sulfur emissions.

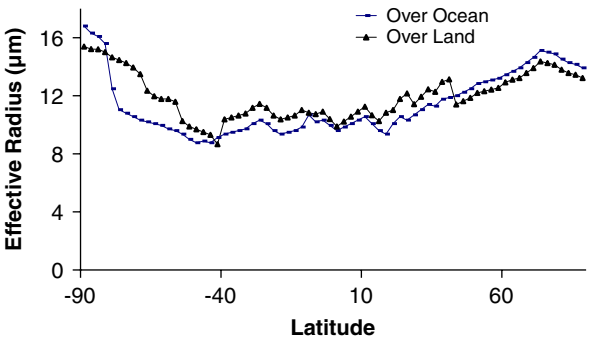

Fig. 4. Simulated latitudinal variations in cloud effective radius.

5. Result and discussions

The respective roles of natural and anthropogenic sources have been first evaluated and later the distributions of sulfate burdens for present-day and pre-industrial periods have been estimated.

Figs. 1 to 3 illustrate the annual mean SO_2 surface concentration, sulfate burden, sulfate AOD distribution for the pre-industrial and present-day emission scenario, respectively. The natural sources are prevalent in both hemispheres with their relative dominance in the Southern Hemisphere (Fig. 1, upper panel). As anthropogenic emissions were negligible during pre-industrial period, the distribution of sulfur species was mainly controlled by natural emissions. An AOD of 0.05 in magnitude can be noted over the oceanic regions in the SH in pre-industrial case. The sulfate burden and AOD dominate NH over the tropics and mid-latitudes where the anthropogenic sources are high (Figs. 2 and 3, lower panels) whereas due to the dominance of biomass sources in the natural case, the higher AOD and sulfate burden could be noted over 10°S–30°S latitude belt. The broad features of these changes are similar to the results of previous studies by Pham et al. (1995), Langner et al. (1992) and Jones et al. (2001). The simulated sulfate loading agrees with magnitude within the estimates provided by previous studies although some variations are likely to appear due to changes in emissions and different formulations of the models.

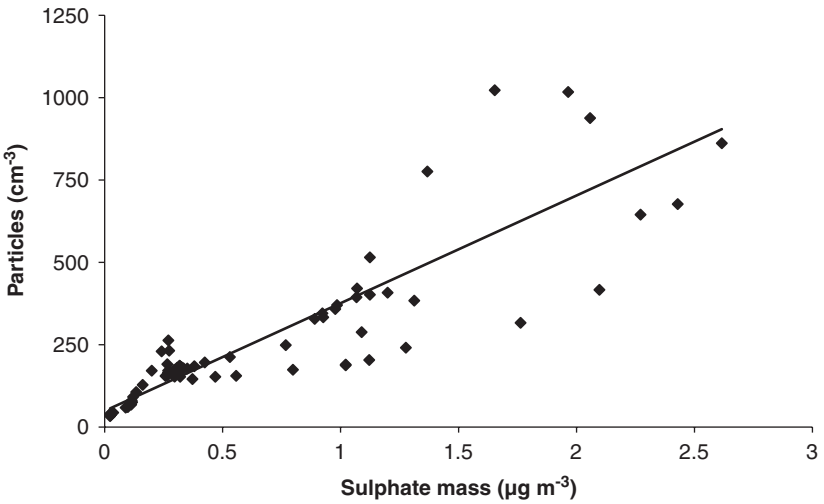

Fig. 5. Number concentration (particles/cm^3) to sulfate mass concentration ratios for the North Atlantic.

The simulated latitudinal variations in cloud droplet effective radii are displayed in Fig. 4. The global mean value from the model is comparable to the observed values given by Han et al. (1994). The agreement between the modeled and observed values is good, with the differences of about 2–3 μm estimated by Han et al. (1994). In general, the cloud droplet radii over land are smaller than of those over the oceans. Thus, the model has correctly simulated in the sense of hemispheric and land-ocean contrast as observed.

For further evaluation, the ratio of the modeled accumulation mode to surface level sulfate in grid boxes over the North Atlantic during the industrial-period are plotted in Fig. 5. The modeled ratio, which lie in the range of 500 ± 250 particles/cm^{-3}, are consistent with the results of Wilson et al. (2001) and van Dingenen et al. (2004). It represents the minimum particle number concentration associated with a given $PM_{2.5}$ loading at clean and rural sites. Particle concentration in this figure refers only to sulfate number concentration in the accumulation mode, while Wilson et al. (2001) gives the value of accumulation mode with combined sea-salt, sulfate accumulation and two mixed mode of BC, OC/sulfate modes.

The simulated latitudinal variations of sulfate AOD and radiative forcing for the pre-industrial

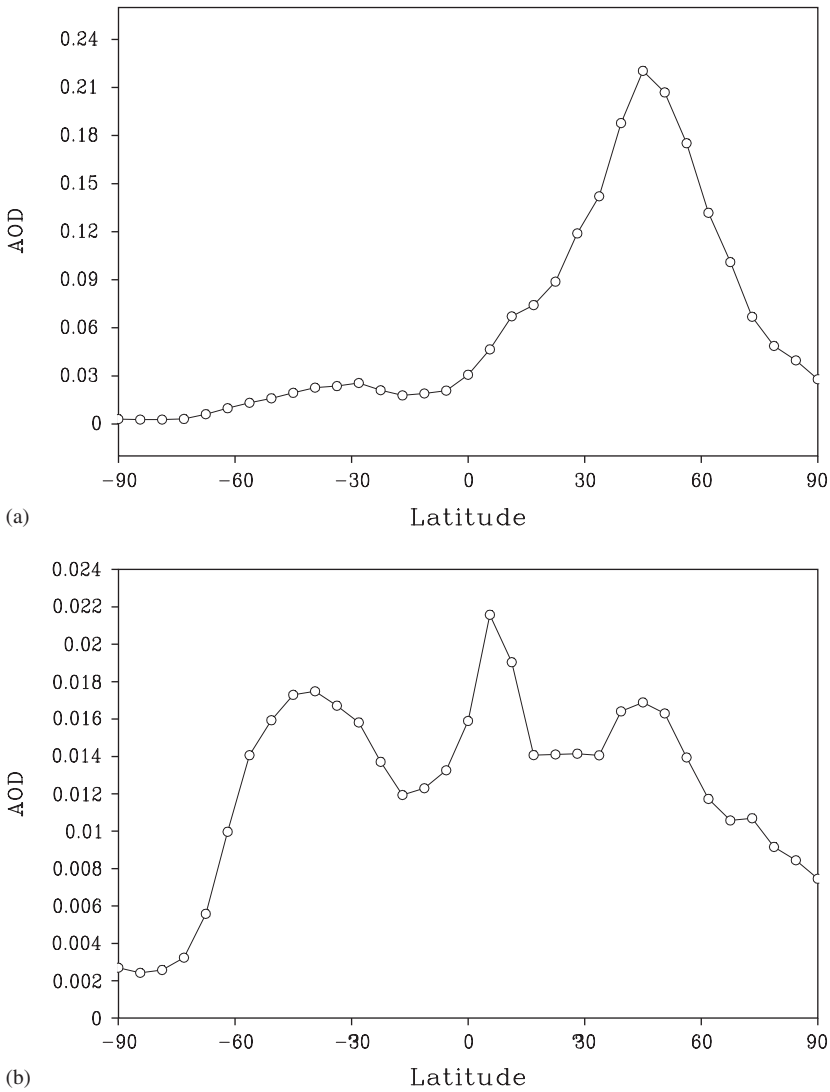

Fig. 6. Simulated latitudinal variations of aerosol optical depth in (a) industrial and (b) pre-industrial simulations.

and present scenario, shown in Figs. 6 and 7 produce a strong NH/SH contrast. As expected, peaks in AOD (Fig. 6a) and direct radiative forcing (Fig. 7a) are observed over the industrialized areas of NH. The maxima of AOD and radiative forcing in pre-industrial case lies in the SH near to the oceanic emission sources. For this 60-month experiment, a total negative radiative forcing (Fig. 7) of $-0.8\,W\,m^{-2}$ in the 30°–60° N latitude band, with somewhat larger values around 50°N($-0.85\,W\,m^{-2}$) has been simulated by the model. The simulated forcing is larger in the NH and increases from $-0.07\,W\,m^{-2}$ in the pre-industrial to $-0.8\,W\,m^{-2}$ in present-day simulations. There is factor 10 increase in the sulfate over this region from pre-industrial time to present day.

Since the indirect forcing is a nonlinear function of changes in droplet size, it is important to model the seasonal cycle of the various cloud parameters for indirect forcing calculations. The annual mean distributions of direct (upper panel) and indirect (lower panel) simulated forcing are shown in Fig. 8. There are forcing maxima adjacent to the main sources of sulfur emission in the North-eastern USA, Europe and China, and also off the west coasts of both North and South America. The spatial distributions for two effects as illustrated in Fig. 8 are quite different. Notably, the direct effect is concentrated in the midlatitudes of the NH and above the continents, but the indirect effect is more widespread with a significant contribution over the oceans. The model simulated annual mean direct

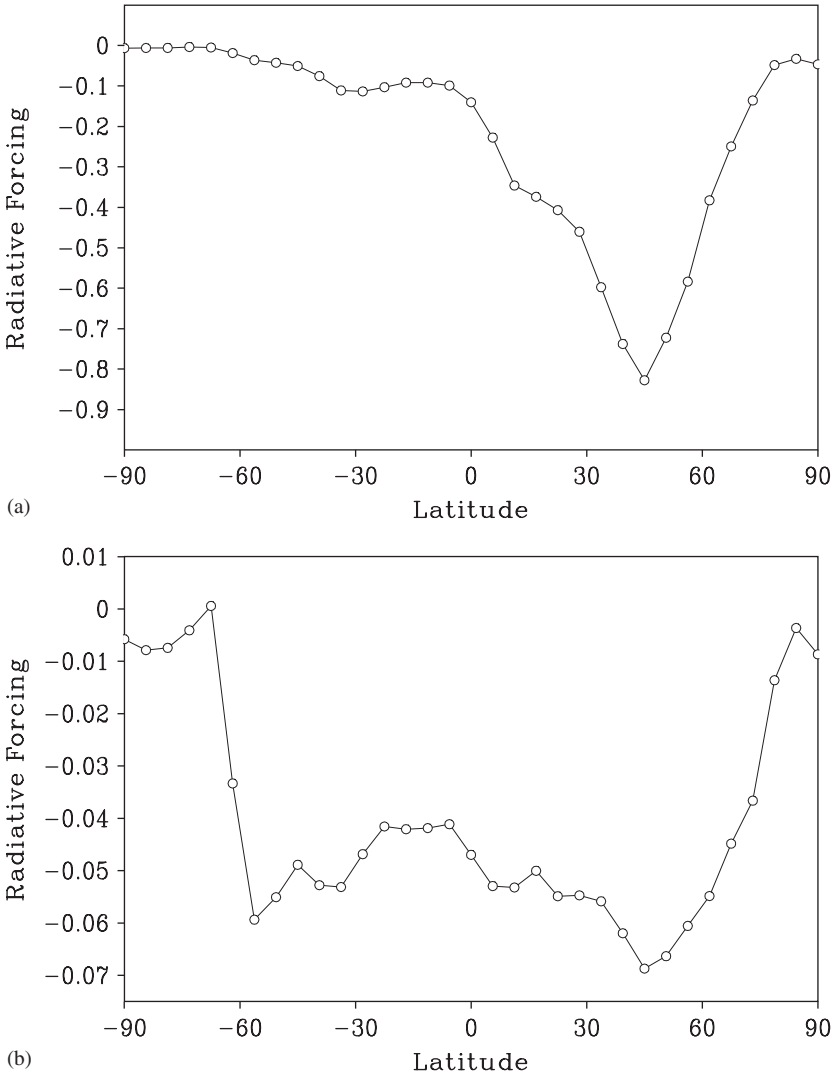

Fig. 7. Simulated latitudinal variations in radiative forcings ($W\,m^{-2}$) (a) industrial and (b) pre-industrial simulations.

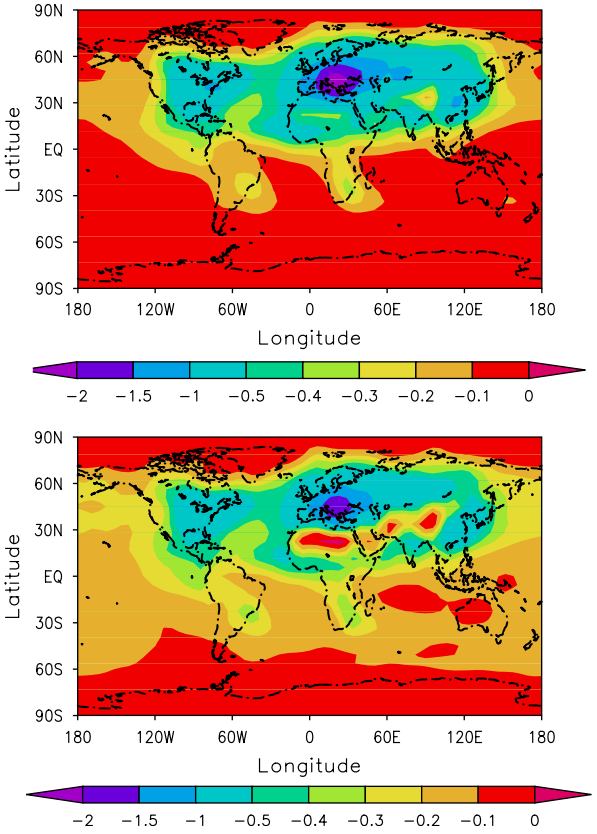

Fig. 8. The simulated global annual mean direct (upper panel) and indirect (lower panel) radiative forcing by sulfate ($W\,m^{-2}$).

radiative forcing ranges from -0.1 to $-1.2\,W\,m^{-2}$, and indirect forcing ranges from -0.4 to $-1.6\,W\,m^{-2}$. The present global annual mean direct forcing is $-0.48\,W\,m^{-2}$, and that of indirect forcing is $-0.68\,W\,m^{-2}$. The current estimate on direct radiative forcing lies in the range of previous (-0.26 to $-0.81\,W\,m^{-2}$) estimates (Ramaswamy et al., 2001). The annual mean global IRF calculated in this study, is at the lower end of previous model estimates (Lohmann and Feichter, 1997; Lohmann et al., 2000; Lohmann, 2004; Lowenthal et al., 2004; Jones et al., 1994; Boucher and Lohmann, 1995; Chuang et al, 1997; Feichter et al., 1997). The discrepancy between present and previous estimates stems from the choice of different formulations and differences in sulfur emissions. The reason for these differences, however, cannot be identified unless sensitivity studies using other parameterization is done.

The prediction of CDNC depends here upon the concentration of sulfate aerosol and varies with the implified cloud properties. Since the aerosol number concentration is largely associated with the radiative changes, it is potentially more useful to relate CDNC to changes in the forcing in the hope of finding the signature of their correlation. The existence of a relationship between aerosol mass and CDNC is also performed using GCM in particular by Boucher and Lohmann (1995).

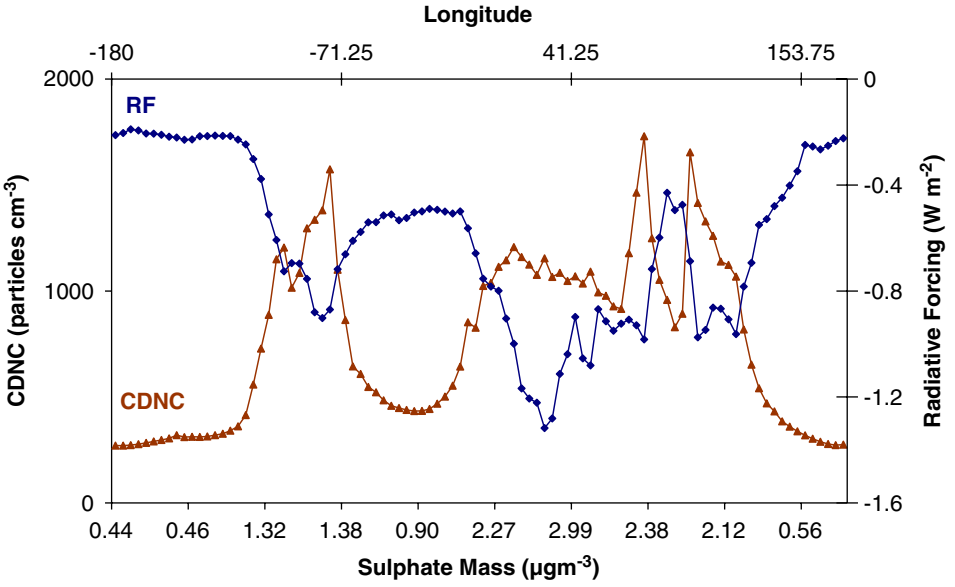

Fig. 9. Longitudinal variations of cloud droplet number concentration (particles cm^{-3}) and indirect radiative forcing ($W\,m^{-2}$) with sulfate mass concentrations.

Fig. 9 shows the longitudinal variations of simulated CDNC and IRF to sulfate mass ratios. The particle size and the associated radiative forcing are proportional to sulfate mass. In general, increase of CDNC with rising aerosol mass, sufficiently correlate. Our results indicate that the expected change in the number concentration is negatively correlated to the IRF. The GCM simulation shows that for the majority of peak occurrence in number and mass concentrations, a very strong overall high negative radiative forcing is estimated. Thus, the minima in radiative forcing correlates well with the maxima in sulfate number and mass concentration.

6. Conclusions

To improve estimates of the radiative forcing by sulfate aerosols, a fully coupled GCM with cloud related properties and aerosol has been used for the study. The first indirect effect is estimated by using the relation of Jones et al. (1994) to determine the CDNC. Facing the great importance to know the role of number concentration, we explored the possibility in indirect forcing estimate derived from model-generated values of sulfate aerosol number concentrations and cloud effective radii.

Model predicts large differences in the sulfate optical depth and direct radiative forcing between pre-industrial to present day simulations. Importantly, the model result indicates that the expected change in the number concentration is negatively correlated to the IRF. The minima in IRF correlate with the maxima in sulfate number and mass concentrations. The model simulated annual mean direct radiative forcing ranges from -0.1 to $-1.2\,W\,m^{-2}$, and indirect forcing ranges from -0.4 to $-1.6\,W\,m^{-2}$. The global annual mean direct effect estimated by the model is $-0.48\,W\,m^{-2}$, and that of indirect is $-0.68\,Wm^{-2}$.

Notably, the presence of other aerosol can also affect the amount of sulfate in the atmosphere. Therefore, for an accurate assessment of sulfate aerosol climate forcing, aerosol components other than sulfates are also required to be included in the model.

Acknowledgement

Authors would like to acknowledge the Indo-French Centre for Promotion of Advanced Research (IFCPAR/CEFIPRA) for their support under project 1911-2. The authors like to thank Institut du Devéloppement et des Ressources en Informatique Scientifique IDRIS)/CNRS to provide computer time for a part of this development work under project 03117. Sincere thanks to Mr Swagata Payra for his time and suggestions, for this paper to take the final shape.

References

Bates, T.S., Lamb, B.K., Guenther, A., Dignon, J., Stoiber, R.E., 1992. Sulfur emissions to the atmosphere from natural sources. Journal of Atmospheric Chemistry 14, 315–337.

Binkowski, F.S., Shankar, U., 1995. The regional particulate matter model: part 1, model description and preliminary results. Journal of Geophysical Research 100, 26191–26209.

Binkowski, F.S., Roselle., S.J., 2003. Models-3 community multiscale air quality (CMAQ) model aerosol component 1 model description. Journal of Geophysical Research 108 (D6), 4183.

Boucher, O., Anderson, T.L., 1995. General circulation model assessment of the sensitivity of direct climate forcing by anthropogenic sulfate aerosols to aerosol size and chemistry. Journal of Geophysical Research 100, 26117–26134.

Boucher, O., Lohmann, U., 1995. The sulfate-CCN-cloud albedo effect: A sensitivity study with two general circulation models. Tellus 47B, 281–300.

Boucher, O., Pham, M., 2002. History of sulfate aerosols radiative forcing. Geophysical Research Letter 29, 9.

Boucher, O., Pham, M., Sadourny, R., 1998. General circulation model simulation of Indian summer monsoon with increasing levels of sulfate aerosols. Annales Geophyscicae 16, 346–352.

Boucher, O., Pham, M., Venkataraman, C., 2002. Simulation of the atmospheric sulfur cycle in the Laboratoire deM′et′eorologie Dynamique general circulation model: model description, model evaluation, and global and European budgets. Note scientifique de l'IPSL no. 23, 32pp.

Chuang, C.C., Penner, J.E., Taylor, K.E., Grossman, ., 1997. An assessment of the radiative effects of anthropogenic sulfate. Journal of Geophysical Research 102, 3761–3778.

Feichter, J., Lohmann, U., Schult, I., 1997. The atmospheric sulfur cycle in ECHAM-4 and its impact on the shortwave radiation. Climate Dynamics 13, 235–246.

Fourquart, B., 1980. Computations of solar heating of the earth's atmosphere: a new parameterization. Atmospheric Physics 53, 35–62.

Han, Q., Rossow, W.B., Lacis, A.A., 1994. Near-global survey of effective droplet radii in liquid water clouds using ISCCP data. Journal of Climate 7, 465–497.

Hauglustaine, D.A., Hourdin, F., Jourdain, L., Filiberti, M.-A., Walters, S., Lamarque, J.-F., Holland, E.A., 2004. Interactive chemistry in the Laboratoire de Météorologie Dynamique general circulation model: description and background tropospheric chemistry evaluation. Journal of Geophysical Research 109, D04314.

Haywood, J.M., Ramaswamy, V., Donner, L.J., 1997a. A limited-area-model case study of the effects of sub-grid scale variations in relative humidity and cloud upon the direct radiative forcing of sulfate aerosol. Geophysical Research Letter 24, 143–146.

Jones, A., Roberts, D.L., Slingo, A., 1994. A climate model study of indirect radiative forcing by anthropogenic sulfate aerosols. Nature 370, 450–453.

Jones, A., Roberts, D.L., Woodage, M.J., Johnson, C.E., 2001. Indirect sulfate aerosol forcing in a climate model with an interactive sulfur cycle. Journal of Geophysical Research 106, 20293–20310.

Kiehl, J.T., Briegleb, B.P., 1993. The relative role of sulfate aerosols and greenhouse gases in climate forcing. Science 260, 311–314.

Langner, J., Rodhe, H., Crutzen, P.J., Zimmermann, P., 1992. Anthropogenic influence on the distribution of tropospheric sulfate aerosol. Nature 359, 712–715.

Le Treut, H., Li, Z.X., Forichon, M., 1994. Sensitivity study of LMD GCM to greenhouse forcing associated with two different cloud water parametrization. Journal of Climate 7, 1827–1841.

Li, Z.X., 1999. Ensemble atmospheric GCM simulation of climate interannual variability from 1979 to 1994. Journal of Climate 12, 986–1001.

Lohmann, U., 2004. Can anthropogenic aerosols decrease the snowfall rate? Journal of Atmospheric Sciences 61, 2457–2468.

Lohmann, U., Feichter, J., 1997. Impact of sulfate aerosols on albedo and lifetime of clouds: a sensitivity study with ECHAM4 GCM. Journal of Geophysical Research 102, 13685–13700.

Lohmann, U., Feichter, J., Penner, J., Leaitch, R., 2000. Indirect effect of sulfate and carbonaceous aerosols: a mechanistic treatment. Journal of Geophysical Research 105, 12193–12206.

Lott, F., 1999. Alleviation of stationary bias in a GCM through a mountain drag parameterization scheme and a simple representation of mountain lift forces. Monthly Weather Review 127, 788–801.

Lowenthal, D.H., Borys, R.D., Choularton, T.W., Bower, K.N., Flynn, M.J., Gallagher, M.W., 2004. Parameterization of the cloud droplet–sulfate relationship. Atmospheric Environment 38, 287–292.

Morcrette, J.J., 1999. Radiation and cloud radiative properties in the European centre for medium range weather forecasts forecasting system. Journal of Geophysical Research 96, 9121–9132.

Pham, M., Muller, J.-F., Brasseur, G., Granier, C., M′egie, G., 1995. A 3-D model study of the global sulfur cycle: contributions of anthropogenic and biogenic sources. Atmospheric Environment 30, 1815–1822.

Ramaswamy, V., et al., 2001. Radiative forcing of climate change in climate change 2001. In: Houghton, J.T., et al. (Eds.), The Scientific Basis, Contribution of Working Group I to the Third Assessment Report of the IPCC. Cambridge University Press, Cambridge, pp. 349–416.

Reddy, M.S., Boucher, O., Venkataraman, C., Verma, S., L′eon, J.-F., Bellouin, N., Pham, M., 2005. GCM estimates of aerosol transport and radiative forcing during INDOEX. Journal of Geophysical Research 109 (D16), D16205.

Sadourny, R., Laval, K., 1984. January and July performances of LMD general circulation model. In: Berger, A. (Ed.), New perspectives in Climate Modelling. Elsevier, Amsterdam, pp. 173–198.

Spiro, P.A., Jacob, D.A., Logan, J.A., 1992. Global inventory of sulfur emissions with $1^\circ \times 1^\circ$ resolution. Journal of Geophysical Research 97, 6023–6036.

Twomey, S.A., 1974. Pollution and the planetary albedo. Atmospheric Environment 8, 1251–1256.

van Dingenen, R., Raes, F., Putaud., Jean-P., et al., 2004. A European aerosol phenomenology—I: physical characteristics of particulate matter at kebside, urban, rural and background sites in Europe. Atmospheric Environment 38, 2277–2561.

Verma, S., Boucher, O., Reddy, M.S., Deb, S.K., Upadhyaya, H.C., Levan, P., Binkowski, F., Sharma, O.P., 2005. Tropospheric distribution of sulfate aerosol number and mass concentrations for INDOEX-IFP and its transport over Indian Ocean. Atmospheric Chemical and Physical Discussion 5, 395–436.

Verma, S., Boucher, O., Reddy, M.S., Upadhyaya, H.C., Levan, P., Binkowski, F., and Sharma, O.P., 2006. Modeling and analysis of sulfate aerosol processes in an interactive chemistry GCM. Journal of Geophysical Research, accepted, 2005JD006077RR.

Wilson, J., Curvelier, C., Raes, F., 2001. A modeling study of global mixed aerosol fields. Journal of Geophysical Research 106, 34081–34108.